Pair distribution function analysis: The role of structural degrees of freedom in the high-pressure insulator to metal transition of VO_2

M. Baldini,[1,*] P. Postorino,[2] L. Malavasi,[3] C. Marini,[4] K. W. Chapman,[5] and Ho-kwang Mao[6,7]

[1]*Geophysical Laboratory, Carnegie Institution of Washington, Advanced Photon Source, Argonne National Laboratory, Argonne, Illinois 60439 USA*

[2]*Dipartimento di Fisica, Universita di Roma Sapienza, P.le A. Moro 4, 00185 Roma*

[3]*Department of Chemistry, University of Pavia and INSTM, Viale Taramelli 16, 27100 Pavia, Italy*

[4]*CELLS-ALBA, Carretera B.P. 1413, Cerdanyola del Valles, 08290, Spain*

[5]*X-Ray Science Division, Argonne National Laboratory, 9700 South Cass Avenue Argonne, Illinois 60439, USA*

[6]*Geophysical Laboratory, Carnegie Institution of Washington, 5251 Broad Branch Road, NW Washington, DC 20015-1305, USA*

[7]*Center for High Pressure Science and Technology Advanced Research, 1690 Cailun Road, Pudong, Shanghai, 201203, People's Republic of China*

(Received 31 July 2015; revised manuscript received 18 May 2016; published 17 June 2016)

The evolution of the local structure of VO_2 was investigated across the pressure-induced insulator to metal transition (IMT) by means of pair distribution function measurements. The pressure behavior of the V-V and V-O bond lengths have been determined. The data demonstrated that the pressure-driven IMT is not activated by the suppression of the Peierls-type distortion. A clear octahedra symmetrization is observed in the metallic phase, suggesting a link between structural degree of freedom and the metallization process.

DOI: 10.1103/PhysRevB.93.245137

The microscopic mechanisms at the origin of the spectacular increase of conductivity in VO_2 is still elusive in spite of being the topic of many theoretical and experimental investigations for more than 50 years. The ultrafast nature of the insulator to metal transition (IMT) creates several possibilities for logic and memory devices, some of which could potentially be transformative [1]. It is therefore crucial to clarify the physics governing such transition from both theoretical and applicative point of view. The IMT is characterized by a change in the resistance of four orders of magnitude near 340 K with a simultaneous structural transition from a monoclinic insulating phase (M1) to a tetragonal (rutile) metallic phase (R) [1]. The monoclinic structure ($P2_1/c$ space group) consists of paired V-atoms displaced out of the octahedral planes, forming V-V dimers tilted with respect to the *a* axis (see right panel of Fig. 1). The R phase shows linear and equally spaced chains of V-atoms. The electronic transition coincides with the structural changes, suggesting a key role of the electron-lattice interactions. The transition is therefore ascribed to the removal of the V-V dimerization along the V-chain [2,3]. On the other hand, theoretical and experimental evidences support the view of VO_2 as a Mott insulator [4–6]. Recent literature suggests that VO_2 should be considered a Peierls-Mott insulator where electron-electron correlations and dimerization of V ions both contribute to the opening of an insulating gap [7,8].

VO_2 can assume several structural phases depending on doping, temperature, and pressure. Two additional insulating phases appears on both applying uniaxial stress [9,10] or doping [11,12]: the monoclinic M2 phase (space group C2/*m*) [13] and the triclinic (T) phase [10,12]. EXAFS measurements carried out on $V_{1-x}Cr_xO_2$ have shed light on the major role of lattice relaxation energy in establishing these competing low-symmetry phases [14]. More recently, it appeared that the common assumption of a direct transition from M1-R will not always apply, and a complex interplay of insulating phases may occur depending of strain [15].

An even more complex scenario has recently emerged from high-pressure (HP) experiments. Indeed, an IMT is also observed applying pressure [16–18]. Optical measurements identifies the onset of this transition at around 10 GPa [16]. Transport data confirm an electronic phase transition [17] and recent results suggest that VO_2 is fully metallic only above 34 GPa [18]. The nature of the P-induced IMT looks remarkably different from the T-induced IMT. The relationship between the structural degrees of freedom and the electronic transition is yet to be fully assessed within an exhaustive framework.

In contrast with the ambient pressure case, where the metallic phase and the rutile structure are closely coupled, HP metallic VO_2 displays different structural properties. A new HP structural phase has been first reported at around 13 GPa by Mitrano *et al.* [19] and recently confirmed [18]. This new structure M1′, which has yet to be fully determined, retains the $P2_1/c$ space group and appears to be a distorted M1 structure [16,18–20]. Above 34 GPa, an additional structural phase, named X, has been recently detected [18].

To get further insight into the HP phases of VO_2 and to clarify the relationship between the structural modification and the P-induced IMT, we investigate the short-range order with a challenging experiment performing x-ray total scattering measurements and atomic pair distribution function (PDF) using a diamond anvil cell [21]. An high-performance experimental setup combined with a careful data analysis allowed us to determine the pressure dependence of the V-V and V-O bond distance, thus providing the first experimental evidence that the removal of V-V dimers is not at the origin of the electronic transition observed at 13 GPa. Nevertheless, our PDF data suggest that a correlation between structural and the electronic degree of freedom still exists in the high-pressure regime.

*Corresponding author: mbaldini@carnegiescience.edu

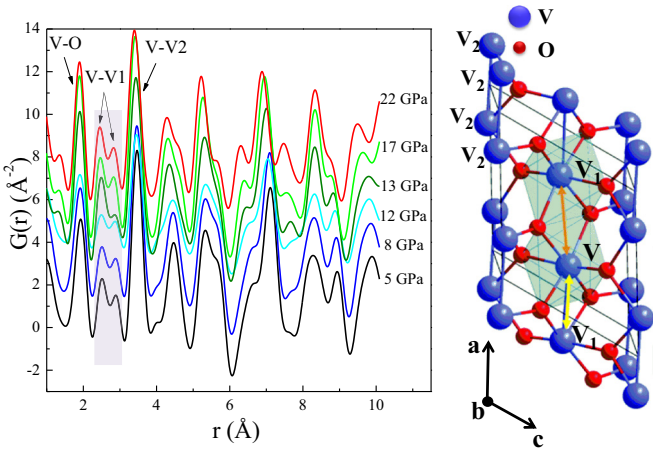

FIG. 1. Extracted $G(r)$ as a function of pressure. The PDFs are scaled up adding a constant to facilitate data visualization. The V-V dimer bond distances are highlighted by the dashed area. The VO_2 structure is reported too. Blue atoms = Vanadium; red atoms = Oxygen. The yellow and orange arrows correspond to the V-V dimer.

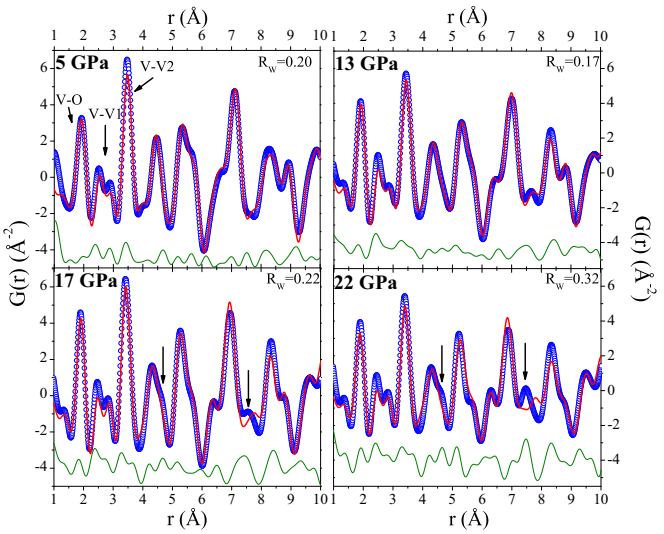

FIG. 2. PDF data at selected pressure: blue circles are used for the extracted $G(r)$, red line indicates the calculated $G(r)$ and the green line is the residual (shifted down to facilitate data visualization). The black arrows in the two bottom plots indicate the PDF features that cannot be modeled using the $P2_1/c$ space group.

In order to perform a high-pressure PDF experiment we fully exploited the technical capabilities recently developed at beamline 11-ID-B at the Advance Photon Source at Argonne National Laboratory. In particular, we took advantage of the new experimental setup that was successfully used to collect high-pressure PDF data up to $Q \geqslant 20$ Å^{-1} [21]. VO_2 powder was prepared by mixing V_2O_3 and V_2O_5 at high temperature with argon gas flow, as described in Ref. [16]. A cross DAC with 300-μm diamond culets and a cell seat with a 70° scattering aperture was employed [22]. The sample was dry-loaded in a 100-μm hole. A dry loading (no pressure medium) avoids further problems in data extraction because of the pressure medium diffraction peaks. The diameter of the x-ray beam was 80 μm. The sample pressure was estimated using the ruby fluorescence method. Total scattering data collected from an empty cell were used to perform the background subtraction. At each pressure, measurements were carried out in multiple exposures ($\lambda = 0.137020$ Å). The 2D data sets were combined and integrated [23] and the Bragg and diffuse scattering from diamonds was identified and masked following the procedure described in Ref. [21]. The corrected total scattering structure function S(Q) was obtained using standard corrections with the software PDFGETX2 [24]. The pair distribution function $G(r)$ was extracted by directly Fourier transforming of the reduced structure function F(Q) up to Q_{max}. Reliable PDF data were obtained up to $Q = 14$ Å^{-1}. Modeling of the experimental PDF data was carried out with the aid of PDFGUI software [25].

The expected M1 structure was observed at ambient pressure with lattice parameters $a = 5.74$ Å, $b = 4.49$ Å, $c = 5.39$ Å, and angle $\beta = 122.6°$. In the M1 structure, the VO_6 octahedra are not regular (see Fig. 1), since there are two different apical V-O bonds and two short and two long equatorial V-O bonds. Because of V-V dimerization (Peiers distortion), V atoms form chains not parallel to the a axis (yellow and orange arrows in Fig. 1) and two different V-V_1 bonds are therefore present: V-V_{1s} = 2.65 Å and V-V_{1l} = 3.12 Å.

In Fig. 1, the extracted $G(r)$s obtained at each pressure are displayed over the 1–10 Å range. The first peak below 2 Å contains the contribution from the V-O pairs, while the two peaks observed between 2 and 3 Å correspond to the V-V_1 bond lengths (dashed area in Fig. 1). Finally, the peak around 3.5 Å contains contributions from V-V_2 bond lengths. No significant changes are observed for the V-O and V-V_2 peaks. The main and the most important evidence is that the V-V_1 distances remain well distinguished up to 22 GPa (as also do the relative intensities of the two peaks), demonstrating that V-V dimers still exist above the structural transition at 13 GPa (M1′ phase). At ambient pressure, the T-driven IMT is characterized by the complete suppression of the V-V dimerization, which takes place with the monoclinic to the rutile structural transition [1]. The P-driven metallization process does not show a strict correlation to the disappearance of the V-V dimers. As a matter of fact, most of the changes are observed above 4 Å and involve interpolyhedra bond lengths. Two shoulders appear, respectively, around 4.5 and 7.5 Å with the onset of the new M1′ phase and become more preeminent as pressure increases.

The PDFs of VO_2 as a function of pressure were modeled with the M1 structure ($P2_1/c$) over the $1 < R < 10$ Å range using lattice parameters obtained from the Rietveld refinement of the average structure. Fitted parameters were the scale factor, the correlation parameters, lattice parameters, atomic positions, and isotropic atomic displacement. In Fig. 2 the extracted $G(r)$ (blue dots) are displayed together with the calculated $G(r)$ (red line) for selected pressures. The M1 model describes very well the features of the PDF data up to 13 GPa. Around 12–13 GPa the structural transition to the HP M1′ phase takes place together with the electronic transition [16–18]. The data collected above this pressure can still be well modeled using the M1 phase confirming that the M1′ phase is a distorted monoclinic structure that retains the $P2_1/c$ space group [18,19]. However, two shoulders fail

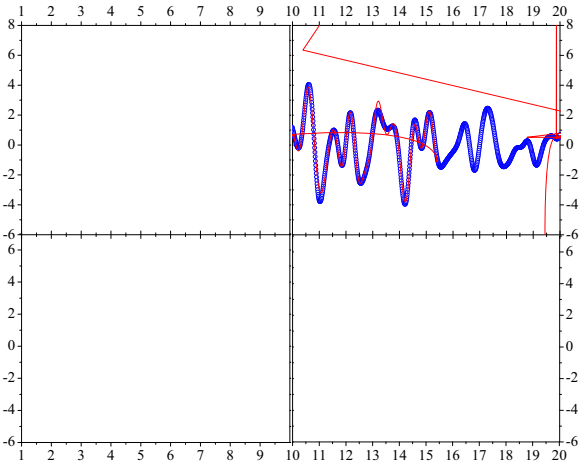
1 2 3 4 5 6 7 8 9 10 11 12 13 14 15 16 17 18 19 20
8 6 4 2 0 -2 -4 -6
6 4 2 0 -2 -4 -6
1 2 3 4 5 6 7 8 9 10 11 12 13 14 15 16 17 18 19 20

of $\delta = 2.5$ at 22 GPa confirms that the V-V dimerization is far from being removed.

The pressure dependence of the V-O atomic distances is displayed in Fig. 5(a). At ambient condition the VO_6 octahedra are orthorhombically distorted. The V-O distances move closer to each other with pressure, indicating a P-driven symmetrization of the VO_6 octahedra. The distortion of the VO_6 was estimated using the equation reported in Ref. [14]. A more pronounced reduction of the octahedral distortion is observed between 0 and 8 GPa. The M1′ phase is thus characterized by more symmetric octahedra [see Fig. 5(b)]. This is also consistent with the pressure dependence of the V-V_2 bond distances [see Fig. 4(c)], which are mostly associated to structural modifications of the octahedra. This pressure behavior remarkably mimics the one observed in the V pre-K-edge peaks of the system, which correspond roughly to the e_g and t_{2g} contributions to the absorption [29]. This result sheds some light on the mechanism behind the IMT in VO_2. Although VO_2 appears to be fully metallic only above 34 GPa in the X structural phase, HP transport data show an electronic transition at 13 GPa with a reduction of the band gap and a resistance change of around 2 orders of magnitude [17,18] (M′ phase). The M1 phase can still be used to refine the high-pressure PDF data. The structural modification affects mostly the medium-range order structure confirming that the M1′ phase is a distorted monoclinic structure [18,19]. Our PDF data show clearly that the VO_6 octahedra are less distorted above 13 GPa and we provided the first experimental evidence that the V-V dimers are still present up to the highest pressure. The removal of the V-V dimerization is therefore not a crucial factor for inducing the electronic transition in VO_2. It was recently discovered that orbital occupation can be controlled by strain in VO_2 thin films [30]. In this case, the IMT temperature is reduced by 60 K in the maximally strained sample. Strain increases the difference between the apical and the equatorial V-O bond length values leading to a change of orbital occupation and to the decrease the IMT temperature [30]. An opposite mechanism may be invoked to explain the effects of pressure on VO_2. The V-O bond distances display a closer distribution above 13 GPa, suggesting that a change in orbital occupation driven by octahedral symmetrization may be at the origin of electronic transition. The octahedral ligand-field splitting affects the hybridization strength between the V $3d$ and the O $2p$ orbitals leading to a different electronic structure arrangement.

In conclusion, we were carrying out a detailed investigation of the evolution of the local structure of VO_2 up to 22 GPa using HP x-ray total scattering measurements and atomic pair distribution function. We provide the first experimental evidence that the V-V_1 dimerization is not suppressed up to 22 GPa. The V-V_1 bond distances remain well distinguished up to 22 GPa, demonstrating that the suppression of the Peierls distortion is not correlated in any way with the change of the electronic properties in the pressure range under investigation. However, at the conductive transformation around 13 GPa, structural modifications of both short and mainly medium-range order do occur. The quantitative data analysis clearly shows an octahedral symmetrization, which appears to be linked with the band-gap reduction. We unambiguously demonstrated that the nature of the P-induced IMT is remarkably different from the T-induced IMT. This result underlines that orbital-lattice coupling plays a significant role in the pressure driven IMT and can represent a severe benchmark for any theoretical *ab initio* calculation devoted to a deeper understanding of the physics of this system.

This work was supported as part of Energy Frontier Research in Extreme Environments Center (EFree), an Energy Frontier Research Center funded by the U.S. Department of Energy, Office of Science under Award No. DE-SC0001057.

[1] Z. Yang, C. Ko, and S. Ramanathan, Annu. Rev. Mater. Res. **41**, 337 (2011).
[2] T. Yao, X. Zhang, Z. Sun, S. Liu, Y. Huang, Y. Xie, C. Wu, X. Yuan, W. Zhang, Z. Wu, G. Pan, F. Hu, L. Wu, Q. Liu, and S. Wei, Phys. Rev. Lett. **105**, 226405 (2010).
[3] A. Cavalleri, Th. Dekorsy, H. H. W. Chong, J. C. Kieffer, and R. W. Schoenlein, Phys. Rev. B **70**, 161102(R) (2004).
[4] Hyun-Tak Kim, Yong Wook Lee, Bong-Jun Kim, Byung-Gyu Chae, Sun Jin Yun, Kwang-Yong Kang, Kang-Jeon Han, Ki-Ju Yee, and Yong-Sik Lim, Phys. Rev. Lett. **97**, 266401 (2006).
[5] M. M. Qazilbash, M. Brehm, Byung-Gyu Chae, P.-C. Ho, G. O. Andreev, Bong-Jun Kim, Sun Jin Yun, A. V. Balatsky, M. B. Maple, F. Keilmann, Hyun-Tak Kim, and D. N. Basov, Science **318**, 1750 (2007).
[6] J. Cao, W. Fan, K. Chen, N. Tamura, M. Kunz, V. Eyert, and J. Wu, Phys. Rev. B **82**, 241101(R) (2010).
[7] S. Biermann, A. Poteryaev, A. I. Lichtenstein, and A. Georges, Phys. Rev. Lett. **94**, 026404 (2005).
[8] C. Weber, D. D. O'Regan, N. D. M. Hine, M. C. Payne, G. Kotliar, and P. B. Littlewood, Phys. Rev. Lett. **108**, 256402 (2012).
[9] J. P. Pouget, H. Launois, J. P. D'Haenens, P. Merenda, and T. M. Rice, Phys. Rev. Lett. **35**, 873 (1975).
[10] Joanna M. Atkin, Samuel Berweger, Emily K. Chavez, and Markus B. Raschke, Jinbo Cao, Wen Fan, and Junqiao Wu, Phys. Rev. B **85**, 020101(R) (2012).
[11] M. Marezio, D. B. McWhan, J. P. Remeika, and P. D. Dernier, Phys. Rev. B **5**, 2541 (1972).
[12] J. P. Pouget, H. Launois, T. M. Rice, P. Dernier, A. Gossard G. Villeneuve, and P. Hagenmuller, Phys. Rev. B **10**, 1801 (1974).
[13] V. Eyert, Ann. Phys. (Leipzig) **11**, 650 (2002).
[14] C. Marini, S. Pascarelli, O. Mathon, B. Joseph, L. Malavasi, and P. Postorino, Europhys. Lett. **102**, 66004 (2013).
[15] A. Tselev, I. A. Luk'yanchuk, I. N. Ivanov, J. D. Budai, J. Z. Tischler, E. Strelcov, A. Kolmakov, and S. V. Kalinin, Nano Lett. **10**, 4409 (2010).
[16] E. Arcangeletti, L. Baldassarre, D. Di Castro, S. Lupi, L. Malavasi, C. Marini, A. Perucchi, and P. Postorino, Phys. Rev. Lett. **98**, 196406 (2007).
[17] X. Zhang, J. Zhang, F. Ke, G. Li, Y. Ma, X. Liu, C. Liu, Y. Han, Y. Ma, and C. Gao, RSC Adv. **5**, 54843 (2015).

[18] L. Bai, Q. Li, S. A. Corr, Y. Meng, C. Park, S. V. Sinogeikin, C. Ko, J. Wu, and G. Shen, Phys. Rev. B **91**, 104110 (2015).
[19] M. Mitrano, B. Maroni, C. Marini, M. Hanfland, B. Joseph, P. Postorino, and L. Malavasi, Phys. Rev. B **85**, 184108 (2012).
[20] C. Marini, E. Arcangeletti, D. Di Castro, L. Baldassare, A. Perucchi, S. Lupi, L. Malavasi, L Boeri, E. Pomjakushina, K. Conder, and P. Postorino, Phys. Rev. B **77**, 235111 (2008).
[21] K. W. Chapman, P. J. Chupas, G. J. Halder, J. A. Hriljac, C. Kurtz, B. K. Greve, C. J. Ruschman, and A. P. Wilkinson, J. Appl. Crystallogr. **43**, 297 (2010).
[22] See Supplemental Material at http://link.aps.org/supplemental/10.1103/PhysRevB.93.245137 for more information about experimental details.
[23] A. P. Hammersley, S. O. Svensson, M. Hanfland, A. N. Fitch, and D. Hausermann, High Pressure Res. **14**, 235 (1996).
[24] X. Qiu, J. W. Thompson, and S. J. L. Billinge, J. Appl. Crystallogr. **37**, 678 (2004).
[25] C. L. Farrow, P. Juhas, J. W. Liu, D. Bryndin, E. S. Bozin, J. Bloch, T. Proffen, and S. J. L. Billinge, J. Phys.: Condens. Matter **19**, 335219 (2007).
[26] L. Malavasi, Dalton Trans. **40**, 3777 (2011).
[27] T. Egami, S. J. L. Billinge, *Underneath the Bragg Peaks: Structural Analysis of Complex Materials* (Pergamon, Amsterdam/Boston, 2003).
[28] A. Mancini and L. Malavasi, Chem. Commun. **51**, 16592 (2015).
[29] C. Marini, M. Bendele, B. Joseph, I. Kantor, M. Mitrano, O. Mathon, M. Baldini, L. Malavasi, S. Pascarelli, and P. Postorino, Europhys. Lett. **108**, 36003 (2014).
[30] N. B. Aetukuri, A. X. Gray, M. Drouar, M. Cossale, L. Gao, A. H. Reid, R. Kukreja, H. Ohldag, C. A. Jenkins, E. Arenholz, K. P. Roche, H. A. Durr, M. G. Samant, and S. S. P. Parkin, Nature Phys. **9**, 661 (2013).